Thermal motion of α-helical molecules in highly crystalline poly(γ-methyl L-glutamate) films

S. Sasaki, Y. Takiguchi, M. Kamata and I. Uematsu
Department of Polymer Chemistry, Tokyo Institute of Technology, Ookayama, Meguro-ku, Tokyo 152, Japan
(Received 6 March 1978; revised 3 August 1978)

Solid films of poly(γ-methyl L-glutamate) were prepared by casting solutions in chloroform, dichloromethane, and *m*-cresol. The mode and amplitude of thermal molecular fluctuations in the crystalline phase were studied by X-ray diffraction. All the films contain α-helical molecules and have hexagonal crystal structures, but differ from each other in their crystallinity and crystallite size. The calculated molecular fluctuation amplitudes also differ considerably. Below a threshold temperature in the range 140°–190°C (different for each sample), the segmental molecular motion is composed of translation along the chain axes coupled with rotation about the axes. At higher temperatures, the structure changes thermoreversibly into a modification, in which a screw-type motion along the α-helix axis is predominant.

INTRODUCTION

Poly(γ-methyl L-glutamate) (PMLG) can exist in various solid state modifications, the structure depending on the casting condition[1,4]. A β-sheet structure is observed in films swollen in formic acid or in crystals precipitated from dilute solution in formic acid[2]. Most other solvents give films with an α-helical conformation. Twisted structures similar to the cholesteric liquid-crystal state of the concentrated solution[5] are retained in films prepared from dichloroethane solution[6,7]. Solutions in *N,N*-dimethylformamide (DMF) at room temperature form a gel which contains fibrous aggregations[8,9]. The poorly-crystalline films obtained from DMF solution may be composed of similarly disordered aggregates. In contrast, the films prepared from solutions in chloroform, dichloromethane (DCM) or *m*-cresol are highly crystalline, and consist of α helices arranged in a hexagonal lattice with dimension $a = 1.19_5$ nm[1,4].

Each of these films of PMLG exhibits a characteristic mechanical behaviour[4,10,11]. Even highly crystalline samples with the same hexagonal structure showed a spread of dynamic mechanical properties, as indicated in *Figure 1*. From the α dispersion (measured at about 180°C) of the film cast from chloroform solution (full line in *Figure 1*), Kajiyama *et al.*[12] concluded that two processes are involved: (1) an α_1 relaxation associated with migrational slip or rotational motion of α helices in the crystalline phase, and (2) an α_2 relaxation associated with the tensile or bending deformation of α helices. Assignment of these as crystalline relaxations is based on the viscous interaction between polymer chains caused by the incoherent lattice vibration[13,14].

In the thermal expansion curves of lattice spacings, a discontinuity was observed at about 140°C for all the films examined[11]. This suggests that the temperature at the onset of incoherent lattice vibration is about 140°C for all cases. However, the average size of the crystallites tends to be larger for films having the α dispersion in the higher temperature range[11]. Therefore, as in the case of polyethylene[15,16], the α dispersion might be related also to viscous slip at grain boundaries, or to defects existing in crystallites[11].

Dynamic mechanical measurements may be used for the investigation of molecular motion, but its interpretation is rather difficult. The intensities of X-ray reflections depend on the mode and decrease with the amplitude of the molecular fluctuations in polymer crystals. In this paper, it is our purpose to deduce the mode and amplitude of segmental vibrations of α helices in the crystalline phase from X-ray diffraction evidence.

EXPERIMENTAL

Materials

A sample of PMLG (Ajicoat A-2000) with viscosity-average molecular weight $M_v \approx 110\,000$ was kindly supplied by Ajinomoto Co. Inc., Japan. Films with thickness 0.1–0.3 mm were obtained by casting the solution in chloroform or dichloromethane (DCM) at room temperature and drying for a few days. These films were labelled as S-CF and S-DCM, respectively. Films were also prepared from *m*-cresol solution by evaporating the solvent at 60° and 100°C for several days (S-M60 and S-M100, respectively). Oriented specimens were prepared by painting the concentrated solution in chloroform or DCM onto a glass plate. All the films were immersed in methyl alcohol for 1 day in order to remove the remaining solvent, and then dried *in vacuo* for several days.

Dynamic mechanical properties of the cast films were measured with a Rheovibron viscoelastometer model DDV-IIC (Toyo Measuring Instrument Co. Ltd, Japan) at a frequency of 110 Hz.

0032–3861/79/010071–05$02.00

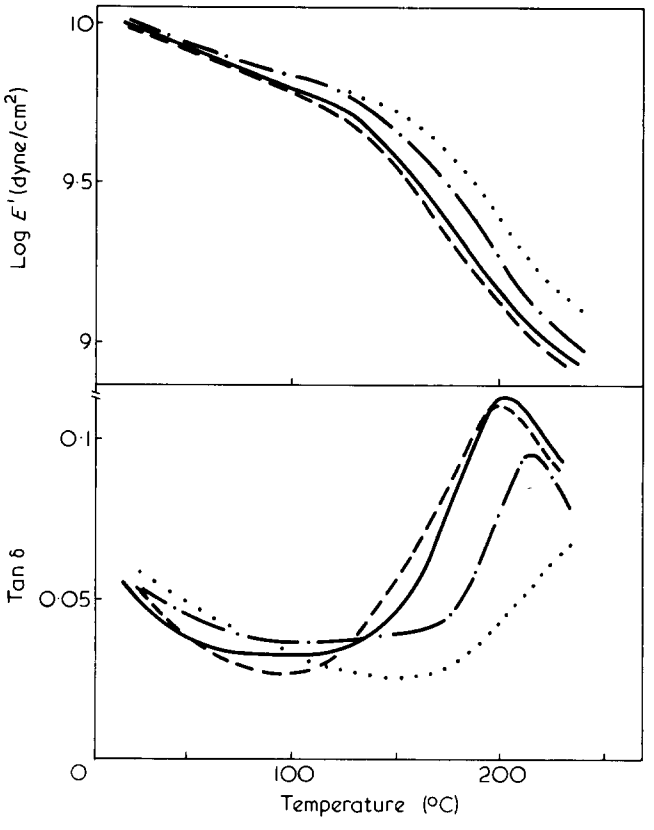

Figure 1 Dynamic mechanical behaviour at 110 Hz for annealed films of poly(γ-methyl L-glutamate) prepared by casting the solutions in chloroform (S-CF, ——), dichloromethane (S-DCM, — — — —), *m*-cresol at 60°C (S-M60, — · —), and *m*-cresol at 100°C (S-M100, · · · ·)

X-ray photographic measurements

The specimens for X-ray diffraction were cut into fine strips with dimensions 10 x 0.3 x 0.3 mm. Wide-angle patterns were recorded on a flat-plate camera or a cylindrical camera, using a Rigaku–Denki X-ray generator with Ni-filtered CuKα radiation. The cast films have a uniplanar orientation, in which the PMLG molecules tend to lie in the film plane[17]. This tendency is also observed for oriented samples. In order to check the orientation, samples were oriented on a sample holder with film surface parallel (EV) and perpendicular to the incident beam.

The high-temperature camera was equipped with inner and outer heaters, by which the temperatures of the sample holder and its surrounding atmosphere were regulated. The two heaters were covered with thin poly(ethylene terephthalate) film through which the diffracted rays were transmitted. For measurements at higher temperatures, samples annealed at 200°C for a few hours were used. The interplanar spacings were calibrated against the 111 reflection of silicon powder sprinkled over the specimen.

Intensity measurements

Reflection intensities were measured from the photographs using a microphotometer, and also by visual comparison with a standard intensity scale. They were measured in each quadrant of a photograph, and simply averaged. Diffractometer data were also collected using a specimen film with dimensions 30 x 20 x 0.2 mm kept firmly in contact with the hot-plate sample holder. Intensity profiles were recorded by a symmetrical reflection technique using a scintillation counter and a pulse height analyser; intensities were measured as the peak area of the diffraction curves.

Determination of reflection width[18]

The integral width of a reflection b as defined by the ratio of peak area to height was obtained from the line profile. By correcting for instrumental broadening b_0 (taken as the width of the 111 reflection of silicon), the true reflection width δs was evaluated in reciprocal space units (nm^{-1}):

$$\delta s = (\cos\theta/\lambda)\,(b^2 - b_0^2)^{1/2} \tag{1}$$

where θ is the Bragg angle and λ the X-ray wavelength.

ANALYTICAL PROCEDURE

Crystallite size and paracrystalline lattice disorder[18]

The samples used in this work are highly crystalline, and have hexagonal crystal structures. Equatorial reflections with $hk0$ indices such as 100, 200 and 300 are clearly observed in the temperature range 25°–200°C. According to Hosemann and Wilke[18], the true integral width of a reflection is determined by the crystallite size and the degree of disorder. On the assumption that the shape factor and the paracrystalline lattice factor in the intensity formula are Lorentzian, the reflection width δs is given as:

$$\delta s_{h00} = \frac{1}{L} + \frac{\pi^2 g_{100}^2 h^2}{\langle d_{100}\rangle} \tag{2}$$

where L is the average crystallite size perpendicular to the chain axes, d_{100} is the spacing of {100} planes, and g_{100} the relative fluctuation:

$$g_{100} = \{\langle d_{100}^2\rangle - \langle d_{100}\rangle^2\}^{1/2}/\langle d_{100}\rangle \tag{3}$$

Accordingly, the size L and the degree of disorder g_{100} can be obtained from a plot of δs vs. h^2.

Thermal fluctuation of α helices in crystals

Models for molecular motion in polymer crystals have been derived using a rigid body approximation for rod-like molecules such as polytetrafluoroethylene[19] and polyoxymethylene[20,21]. The α-helical conformation of polypeptides also is very stiff. Segmental motion in these molecules may comprise three types of fluctuations: (a) translational displacement of chain segments along their axes, (b) rotation about their axes and (c) screw displacement[19]. The length of the vibrating segment depends generally on the intra- and intermolecular force constants[13,14].

The intensity of an hkl reflection I_{hkl}^0 at a reference temperature (25°C) decreases to I_{hkl}^T at a higher temperature. The motion of the PMLG chain should be negligibly small at 25°C, since the reflection intensities do not change very much below 100°C. According to Clark and Muus[19], the following relation can be derived for a helical polymer:

$$I_{hkl}^T = I_{hkl}^0 \exp(-B_l) \tag{4}$$

and

$$B_l = 4\pi^2(l/c)^2\langle\Delta z^2\rangle + n^2\langle\Delta\phi^2\rangle - 4\pi n(l/c)\langle\Delta z\Delta\phi\rangle \tag{5}$$

where $\langle \Delta z^2 \rangle$ and $\langle \Delta \phi^2 \rangle$ are mean square amplitude of translation and that of rotation, c is the axial repeat distance 2.70 nm, and n the lowest order of Bessel function in the structure factor formula[22]. For the 18-residue 5-turn α helix, the lowest values of n are 0, 4, −3 and 1 for the layer lines l = 0, 2, 3 and 5, respectively.

From this relationship, the following qualitative interpretation can be derived[19]. (1) Translation along the chain axes lowers the reflection intensities for higher layer lines. (2) Rotation about the axes weakens the reflections on layer lines with a large value of n. (3) $\langle \Delta z \Delta \phi \rangle = 0$ if there is no correlation between the translational and rotational motions. (4) No motion affects the equator ($B_{l=0} = 0$). (5) Screw motion along the α helix axis has no effect for the 5th layer line, since $\Delta z = (c/5)(\Delta\phi/2\pi)$ and therefore $B_{l=5} = 0$).

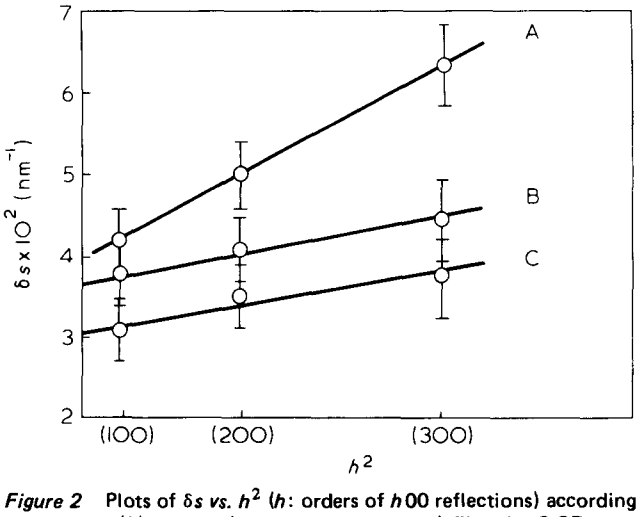

Figure 2 Plots of δs *vs.* h^2 (h: orders of $h00$ reflections) according to equation (2) for poly(γ-methyl L-glutamate) films for S-CF (S-DCM) (A); S-M60 (B) and S-M100 (C)

RESULTS AND DISCUSSION

Crystallite size and lattice disorder

The integral widths of $hk0$ reflections were found to be nearly independent of temperature over the range 25°–200°C. *Figure 2* shows the plots of δs vs. h^2, from which the average lateral dimension of crystallite L and the paracrystalline disorder g_{100} were calculated (*Table 1*). The crystallinity and the crystallite size are similar in magnitude for S-CF and S-DCM. Samples of the S-M series have a small value of g_{100}, being different in crystallite size which depends on the casting temperature. The high α dispersion temperature for the S-M series (*Figure 1*) should be partly attributable to their high crystallinity and large crystallite size.

Table 1 Crystallite lateral size L and paracrystalline disorder g_{100} of poly(γ-methyl L-glutamate) films

Sample	Casting solvent	Casting temperature (°C)	L (nm)	g_{100} (%)
S-CF	Chloroform	Room temp.	25	1.7
S-DCM	Dichloromethane	Room temp.	25	1.7
S-M60	*m*-Cresol	60	28	1.0
S-M100	*m*-Cresol	100	33	1.0

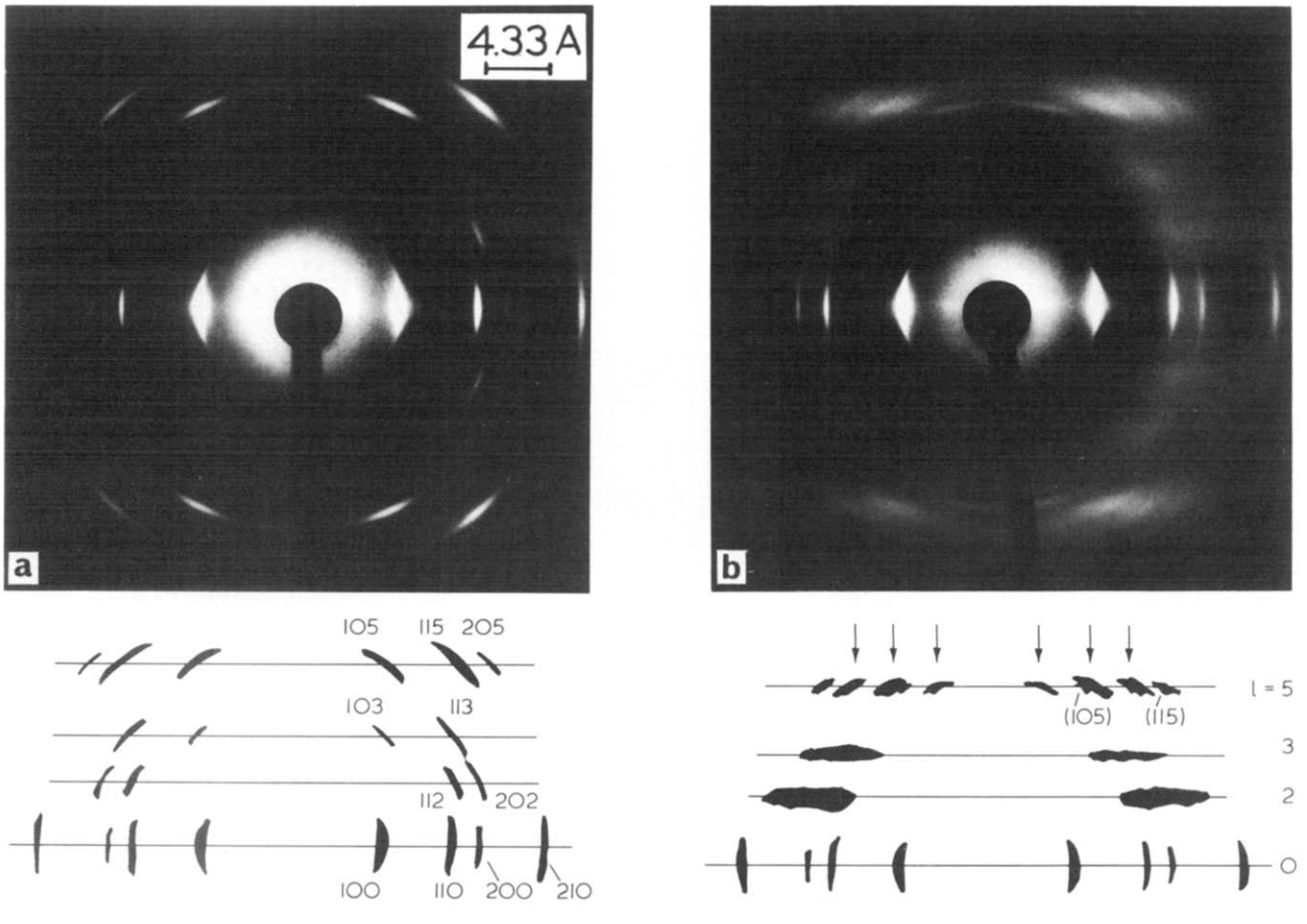

Figure 3 X-ray EV patterns and their schematic diagrams for an oriented S-CF film of poly(γ-methyl L-glutamate) taken at (a) 25°C and (b) 170°C

Thermoreversible structure transition at high temperatures

Figure 3 shows the X-ray patterns of the oriented S-CF sample taken at 25° and 170°C and their schematic diagrams. The equatorial spots are quite sharp at higher temperatures; the molecular packing is strictly hexagonal in axial projection (the cell dimension $a = 1.24_3$ nm at 200°C). The observed and calculated spacings are listed in *Table 2*. The α-helical conformation is maintained at higher temperatures, since the 18th meridional reflection of spacing 0.15 nm can be observed at 200°C. The Bragg spots on the 2nd and 3rd layer lines are observable at 160°C, but disappear into continuous streaks at 170°C (*Figure 3b*). The reflections on the 5th layer line also disappear at about 160°C (in the case of S-CF), while new reflections indicated by arrows begin to appear in the same temperature range.

The overall intensity of the 5th line decreases with rising temperature. The pattern at temperatures higher than 170°C comprises the Bragg spots on the 0th and 5th layer lines and continuous streaks on the 2nd and 3rd lines. As mentioned in a preceding section, this feature suggests that the screw motion along the α-helix axis is predominant. As a result of this motion, the α-helix is regarded as an electron dense rope of pitch 0.54 nm. The new reflections occur thermoreversibly at $\xi \approx 0.004$, 0.10 and 0.013 nm^{-1} on the 5th layer line and may clearly be seen even at 200°C, where ξ is the radial coordinate in the reciprocal space. Since the equatorial reflections characteristic of the hexagonal lattice (*Table 2*) occur at $\xi = 0.0093$, 0.0161, 0.0186 nm^{-1} and so on, a triclinic unit cell (with dimensions $a = b = 1.25$ nm, $c' = 0.54$ nm, $\alpha = \beta = 96°$, and $\gamma = 119°$ at 200°C) may be introduced in order to explain the new reflections. The triclinic unit cell seems a little strange in view of steric repulsion between neighbouring chains. A particular kind of correlation may exist among the respective molecular motions, offering an explanation for the 5th layer line. The analysis is difficult on the present X-ray data.

The new reflections on the 5th layer line begin to appear at about 140°C for S-DCM, 190°C for S-M60, and 200°C for S-M100 (*Figure 4*).

Table 2 Observed and calculated spacings of X-ray reflections for the PMLG film S-CF at 200°C

hkl	d_{obs} (nm)	d_{calc} (nm)*
100	1.08	1.077
110	0.623	0.622
200	0.539	0.538
210	0.407	0.407
300	0.359	0.359
$l = 5$	0.53	
$l = 5$	0.47_5	
$l = 5$	0.44	

* The calculation is based on a hexagonal lattice with dimensions $a = 1.24_3$ nm

Molecular motion of α helices in crystals

The X-ray data for the oriented S-CF sample are essentially equivalent to those for the cast film. The same situation appears to occur for the S-DCM samples. The remarkable change of X-ray pattern is observed at about 160°C for S-CF (*Figure 3*), 140°C for S-DCM, 190°C for S-M60, and 200°C for S-M100 (*Figure 4*). The transition temperature as well as the molecular motion is different for each sample.

The temperature dependence of intensity was measured for the reflections on the 2nd, 3rd and 5th layer lines below the respective transition temperatures. The mean-square amplitudes $\langle \Delta z^2 \rangle$ and $\langle \Delta \phi^2 \rangle$ were calculated according to equations (4) and (5), and plotted in *Figure 5*. The errors were estimated from those in intensity measurements of about 10%. The cross-term $\langle \Delta z \Delta \phi \rangle$ could not be neglected for each case. On the assumption that the pitch of the screw

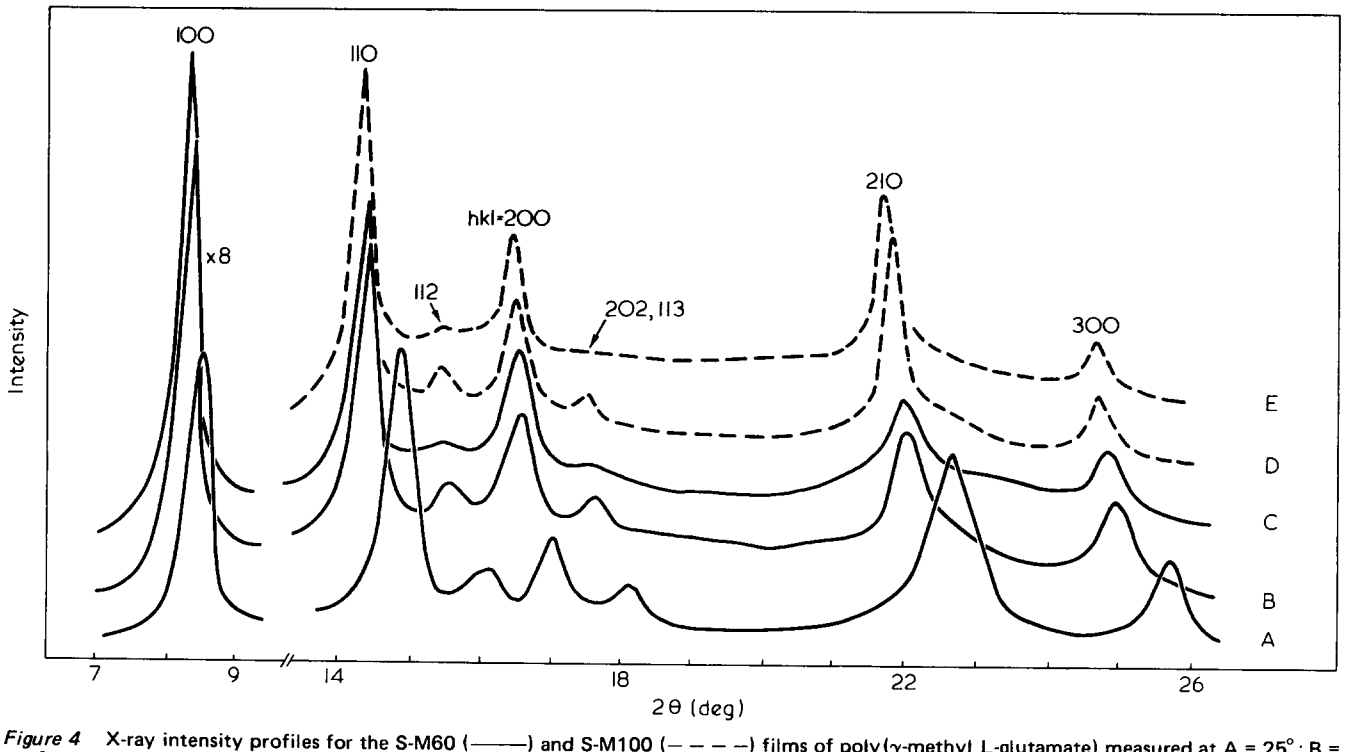

Figure 4 X-ray intensity profiles for the S-M60 (———) and S-M100 (— — — —) films of poly(γ-methyl L-glutamate) measured at A = 25°; B = 170°, C, D = 190° and E = 200°C

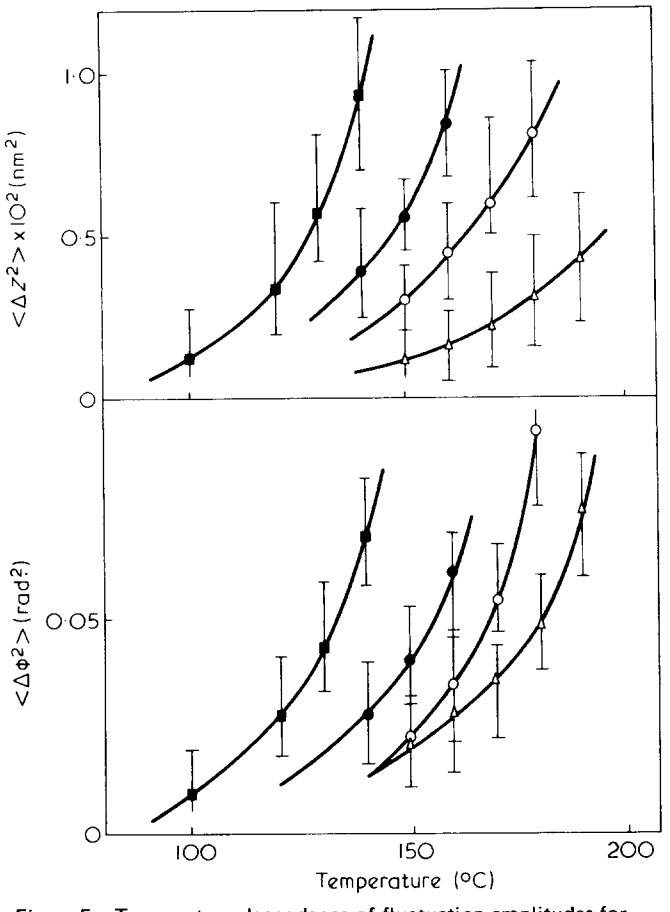

Figure 5 Temperature dependence of fluctuation amplitudes for poly(γ-methyl L-glutamate) films (see text). ■, S-DCM; ●, S-CF; ○, S-M60; △, S-M100

motion is equal to the helix pitch $P = 0.54$ nm, the translational component due to the screw motion, $\langle\Delta z^2\rangle_s = \langle\Delta z\Delta\phi\rangle(P/2\pi)$, was calculated as less than 15% of $\langle\Delta z^2\rangle$. On the other hand, the librational component, $\langle\Delta\phi^2\rangle_s = \langle\Delta z\Delta\phi\rangle(2\pi/P)$, could not be well-defined, since it was distributed in the range 0–200% of $\langle\Delta\phi^2\rangle$. Therefore, it is concluded that the molecular motion in the PMLG crystals is composed of translation along the axes coupled partly with rotation about the axes. Above the transition temperatures, the molecular motion is essentially of the screw type along the α helix axis, as mentioned before.

The temperature dependence of the X-ray patterns indicates that these molecular motions are not localized in defects but occur in crystalline regions. The great difference in the thermal motion must be attributed to the crystallite itself. The spacing of each reflection, however, is the same for all the samples within the experimental error in the whole temperature range. Furthermore, the spacings of equatorial reflections have a discontinuity around 140°C in the thermal expansion curves[10,11]. The onset of the incoherent lattice vibration occurs at about 140°C for each sample despite the different amplitudes. Generally, the crystallite size and the degree of crystallinity influence the lattice vibration and the mechanical properties. The samples S-CF and S-DCM exhibit similar mechanical behaviour (*Figure 1*) and crystallite size (*Table 1*). However, the molecular motion deduced from X-ray data is different (*Figure 5*). The mechanical α dispersions are observed at temperatures higher than the structure transition temperatures. Therefore, the molecular motion is much enhanced at the α dispersion temperatures, including the transition of molecules from an interchain potential minimum to another over the barrier between them. Such a large-scale motion may be attained at the same temperature for S-CF and S-DCM. Another possibility is that the α dispersion may not be related to the incoherent lattice vibration, but could, for instance, be related to viscous slip at grain boundaries. For the S-M series, the fluctuation amplitudes are small in comparison with those for S-CF and S-DCM. This situation is probably due to their high crystallinity and large crystallite size.

Molecular motions in polymer crystals have usually been discussed under the boundary condition of fixed ends. With this condition, the amplitudes should increase with the crystallite thickness, as found in the cases of polyethylene and *n*-alkanes[13–15,23]. In contrast, the amplitudes decrease with increasing crystallite thickness under a free boundary condition. In this work, the crystallite thickness along the chain axes could not be estimated, but it is presumably larger for samples with long lateral dimensions. From the results shown in *Table 1* and *Figure 5*, the behaviour in PMLG is opposite to that of polyethylene. The segmental molecular motion in the PMLG crystals must take place substantially under a free boundary condition.

REFERENCES

1 Bamford, C. H., Brown, L., Elliott, A., Hanby, W. E. and Trotter, I. F. *Nature* 1952, **169**, 357
2 Nakajima, A., Fujiwara, T., Hayashi, T. and Kaji, K. *Biopolymers* 1973, **12**, 2681
3 Mohadger, Y. and Wilkes, G. L. *J. Polym. Sci. (Polym. Phys. Edn)* 1974, **14**, 963
4 Watanabe, J., Sasaki, S. and Uematsu, I. *Polym. J.* 1977, 9, 451
5 Robinson, C. *Mol. Cryst.* 1966, **1**, 467
6 Tachibana, T. and Oda, E. *Bull. Chem. Soc. Jpn* 1973, **46**, 2583
7 Watanabe, J., Sasaki, S. and Uematsu, I. *Polym. J.* 1977, 9, 337
8 Ishikawa, S. *J. Polym. Sci. (A)* 1965, **3**, 4075
9 Blais, J. J. B. P. and Geil, P. H. *J. Ultrastructure Res.* 1968, **22**, 303
10 Watanabe, J., Naka, M. and Uematsu, I. *Rep. Prog. Polym. Phys. Jpn* 1977, **20**, 621
11 Watanabe, J., Naka, M., Watanabe, J., Watanabe, K. and Uematsu, I. *Polym. J.* 1978, **10**, 569
12 Kajiyama, T., Kuroishi, M. and Takayanagi, M. *J. Macromol. Sci. (B)* 1975, **11**, 121
13 Peterlin, A., Fischer, E. W. and Reinhold, C. *J. Chem. Phys.* 1962, **37**, 1403
14 Okano, K. *J. Polym. Sci. (C)* 1966, **15**, 95
15 Tsuge, K., Enjoji, H., Terada, H., Ozawa, Y. and Wada, Y. *Jpn J. Appl. Phys.* 1962, **1**, 270
16 Iwayanagi, S. and Miura, I. *Ibid.* 1965, **4**, 94
17 Ito, K., Kajiyama, T. and Takayanagi, M. *Polym. J.* 1977, 9, 355
18 Hosemann, R. and Wilke, W. *Makromol. Chem.* 1968, **118**, 230
19 Clark, E. S. and Muus, L. T. *Z. Krist.* 1962, **117**, 108, 119
20 Chiba, A., Hasegawa, A., Hikichi, K. and Furuichi, J. *J. Phys. Soc. Jpn.* 1966, **21**, 1777
21 Tanaka, S. *Ibid.* 1974, **36**, 1096, 1395
22 Cochran, W., Crick, F. H. C. and Vand, V. *Acta Crystallogr.* 1952, **5**, 581
23 Tsuge, K. *Jpn J. Appl. Phys.* 1964, **3**, 588